Available online at www.sciencedirect.com
SCIENCE DIRECT®
Journal of Theoretical Biology 240 (2006) 501–510
Journal of Theoretical Biology
www.elsevier.com/locate/yjtbi

Estimating conductances of dual-recorded neurons within a network of coupled cells

Pierre A. Fortier[a,*], Maimouna Bagna[b]

[a]Department of Cellular & Molecular Medicine, University of Ottawa, Canada K1H 8M5
[b]Faculty of Engineering, University of Ottawa, Canada K1N 6N5

Received 27 May 2005; received in revised form 30 August 2005; accepted 17 October 2005
Available online 28 November 2005

Abstract

Simultaneous pre- and postsynaptic cell recordings are used to calculate gap junction conductance based on an equivalent electrical circuit of an electrically coupled pair of cells. This calculation is imprecise when recording from a cell pair that is coupled to neighboring cells providing indirect conductance paths between the recorded cells. Despite this imprecision, junctional conductance has been calculated for coupled cell networks during the past 40 years since a more accurate method was lacking. The present study simulated a three-dimensional network of electrically coupled heterogeneous neurons and used mathematical modeling to reduce the complexity to the simplest equations that could more accurately estimate the electrical properties of dual-recorded cells in the network. Analyses of the simulations showed that knowledge of the number of unrecorded cells directly linked to the recorded cells and of the voltage responses of these recorded cells were largely sufficient to accurately predict the direct junctional resistance linking the recorded cells as well as the input resistance of the recorded cells that would exist in the absence of junctional coupling. All model parameters could be obtained from real dual-intracellular penetrations which allow electrophysiological recordings and intracellular staining.

Keywords: Gap junction; Electrical synapse; Electrotonic coupling; Junctional conductance; Neural network; Input resistance

1. Introduction

A gap junction is an intercellular channel allowing the exchange of ions and molecules less than 16 Å in diameter for communication between cells (Elenes et al., 2001; Rozental et al., 2000; Simon and Goodenough, 1998). Gap junctions are normally clustered forming plaques consisting of just a few to several thousand junctions (Rouach et al., 2002). The electrotonic coupling of neurons by gap junctions confers properties for communication in nervous tissues beyond that provided by chemical synapses. These properties include greater speed of synaptic relay, transmission of subthreshold potentials, reciprocal communication, coincidence detection, synchronization of neurons, and oscillation (Bennett, 1997; Marder, 1998).

The most direct and arguably the only convincing experiments to show the existence of functional electrical synapses involve simultaneous recordings from pairs of connected cells (Bennett, 1997; Galarreta and Hestrin, 2001, 2002). The equations to quantify the electrical coupling during current-clamp recordings were derived about 40 years ago by Bennett (Bennett, 1966, 1977) using an equivalent circuit model of two coupled cells. These equations provide accurate estimates of electrical coupling during dual-recordings from isolated pairs of real cells (Clapham et al., 1980; Spray et al., 1981; Veenstra, 2001) because these conditions are equivalent to those of the model used in deriving the equations for electrical coupling. The limitations of these equations were partially described in the original paper but, for lack of a better method, they have been used since then to calculate the electrical properties of gap junctions linking pairs of recorded cells even though many of these cells form part of highly interconnected networks (Galarreta and Hestrin, 2001; Neyton and Trautmann, 1985). In such networks of

*Corresponding author. Tel.: +1 613 562 5800x8147; fax: +1 613 562 5434.
E-mail address: pfortier@uottawa.ca (P.A. Fortier).

0022-5193/$ - see front matter © 2005 Elsevier Ltd. All rights reserved.
doi:10.1016/j.jtbi.2005.10.009

coupled cells, the electrical properties obtained from dual-cell recordings would not only reflect the recorded cell pair but also that of the unrecorded surrounding cells to which they are connected by gap junctions.

A recent study (Amitai et al., 2002) used a system of steady-state equations to evaluate coupling among simulated neurons with *homogeneous* electrical properties in simple networks (one- and two-dimensional architectures possibly representing a column and a layer of electrically coupled neurons) whose architectures were suggested from in vitro results of cell density and coupling coefficients for a sample of cell pairs in a network. Their overall objective was to estimate the average summed coupling conductance that each cell receives from all of its neighbors but as an aside they provided a rough estimate of the conductance linking dual-recorded cells which lay somewhere within 0.36–2 nS or 500–2800 MΩ for a specific test case. These conductance parameters are difficult to estimate accurately and a practical solution to this problem would be welcomed by electrophysiologists.

The overall objective of the present study was to provide a simple and accurate estimate of the conductance linking dual-recorded cells within biologically relevant architectures of coupled cells. This was done using a simulation program with integrated circuit emphasis (SPICE) to create a three-dimensional (3D, representing several cell layers) network of neurons with *heterogeneous* electrical properties that were fully randomized within known biological values. Mathematical modeling was then used to reduce the complexity to the simplest equations, based only on parameters available during dual-cell recordings, that could accurately quantify the direct conductances between cell-pairs recorded from the simulated networks. Equations were also derived to extract the resistance of a recorded neuron from its input resistance which comprised both neuron and junctional resistances. These derivations extend Bennett's approach (Bennett, 1966, 1977) beyond its limitations for dual-recorded cells embedded in a network of coupled cells. Our equations provided relatively accurate estimates of membrane properties using only data that are available from real dual-intracellular penetrations which allow both electrophysiological recordings and intracellular staining with dyes that diffuse through gap junctions to reveal connectivity.

2. Methods

2.1. Notation

The notation used in this study is based on Bennett's classic papers (Bennett, 1966, 1977) defining a circuit model of coupled cells. I is current, V is voltage, and R is resistance. Injection of current into one of two coupled cells will be affected by the resistance of each cell and the gap junction resistance linking the pair of cells. To distinguish between these components, a one-letter subscript indicates the location among a recorded pair of electrotonically coupled cells: R_1 is the resistance of cell 1, R_2 is the resistance of cell 2, R_j is the junctional resistance linking cells 1 and 2, I_1 is the current injected into cell 1, and I_2 is the current injected into cell 2. The first letter of a two-letter subscript indicates where the current was applied: V_{11} is the voltage in cell 1 due to stimulation in cell 1, V_{12} is the voltage in cell 2 due to stimulation of cell 1, V_{22} is the voltage in cell 2 due to stimulation in cell 2, V_{21} is the voltage in cell 1 due to stimulation of cell 2, R_{11} is the input resistance of cell 1 measured during stimulation of cell 1, and R_{22} is the input resistance of cell 2 measured during stimulation of cell 2.

The equations used to derive the gap junction and neuron resistances were based on the simultaneous recording of 2 coupled cells in a network. The subscript "p" was used to indicate the contribution of neighboring cells coupled in parallel as described here for the junctional resistance: R_j is the junctional resistance resulting from the direct connection between the recorded-cell pair and R_{j_p} is the parallel junctional resistance resulting from both the direct connection between the recorded-cell pair and the indirect parallel connections through neighboring cells. Other less commonly used variables are defined where they first appear in the text.

2.2. Simulations using SPICE

The implementation of SPICE used in this study was from OrCad Inc. (Beaverton, Oregon). This simulation software allowed us to define an equivalent circuit of electrotonically coupled cells and then to view the voltage changes and current flow in response to intracellular current injections. Values from published data were used for the neuron resistances (Pare et al., 1998), junctional resistances (Galarreta and Hestrin, 2001), and injected currents (Galarreta and Hestrin, 1999; Gibson et al., 1999; Pare et al., 1998; Tamas et al., 2000) that were simulated in SPICE. The resting potential of cells was assumed to be 0 mV in order to simplify calculation of the voltage response to current injection. The responses of these simulated neurons and their network architecture were used to develop equations that could be applied to intracellular studies in real neurons in order to estimate the junctional resistance between dual-recorded neurons as well as the resistance contributed by each of these neurons. The steps in the derivation of all equations were verified using Maple software which is a symbolic computation system (Waterloo Maple Inc., Waterloo, Ontario, Canada) and the accuracy of these equations were estimated from their ability to reveal the known resistances used in the simulated 3D neural networks of electrically coupled heterogeneous cells.

3. Results

3.1. Three-dimensional simulation of coupling

The basic architecture of the simulated 3D network is shown in Fig. 1 using cuboidal-shaped cells to simplify the

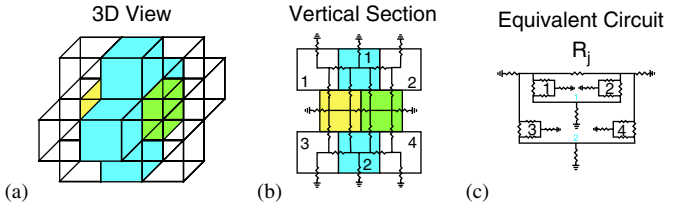

Fig. 1. Architecture of a 3D network of coupled cells with direct and indirect pathways for current flow between neighboring cells. (a) A 3D view showing the direct connection between dual-recorded cells (yellow and green) and indirect connections via a single interposed blue cell or via several transparent and blue cells. For clarity, the transparent cells to the left and right of the recorded cells are not drawn in this illustration of one layer of cells surrounding the dual-recorded cells. (b) A vertical section through the network to reveal the underlying circuitry formed of neuron and junctional resistances. Only resistances of the cell leading to the extracellular space (represented by the ground) and of the gap junctions leading to the intracellular spaces of connected cells were simulated. Membrane capacitance, which delays reaching steady-state, was not simulated since only steady-state values were recorded. (c) The circuitry is redrawn as a simplified equivalent circuit with the junctional resistance between the dual-recorded cells identified by R_j. The blue and black numbers represent the corresponding blue and transparent cells which form primary and secondary loops for current flow between the dual-recorded cells.

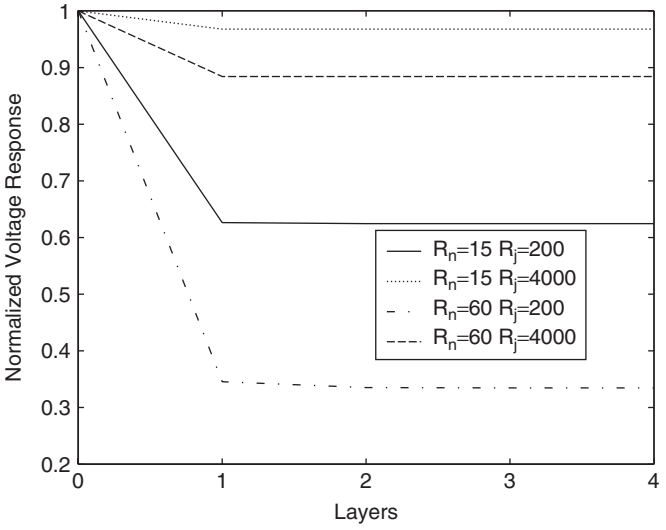

Fig. 2. Effects of adding layers of cells, around the recorded cell pair, on the voltage responses to −1.0 nA current injection. Voltage responses were normalized to the values obtained with 0 layers (i.e. isolated pair of coupled neurons). All cells had the same neuron resistance (R_n) and junctional resistance (R_j), so the voltage responses were identical for current injections into either of the two recorded neurons. Four extreme conditions were tested (1) $R_n = 15$ and $R_j = 200\,\mathrm{M\Omega}$, (2) $R_n = 15$ and $R_j = 4000\,\mathrm{M\Omega}$, (3) $R_n = 60$ and $R_j = 200\,\mathrm{M\Omega}$, and (4) $R_n = 60$ and $R_j = 4000\,\mathrm{M\Omega}$.

illustration of dual-recorded cells surrounded by one layer (a layer represents all the cells forming a single cell thick envelope) of cells. All neighboring cells were coupled by gap junctions. Although the blue cells appear to be independent from one another, they become linked by a single intermediate cell when another layer of cells is added. Less than four layers of cells surrounding the centrally located recorded pair of cells (yellow and green) were simulated because the voltage responses to injection of hyperpolarizing currents were mostly affected by adding the first layer of cells but changed little with networks of up to three layers and were completely unaffected by additional layers (Fig. 2). The four lines in Fig. 2 represent four conditions which covered all combinations of the extreme ranges of neuron and junctional resistances (Galarreta and Hestrin, 1999; Gibson et al., 1999; Pare et al., 1998; Tamas et al., 2000). It can be seen that adding one layer produced a decrease in the voltage responses for all four conditions but the largest relative voltage drops occurred for the lowest junctional resistance ($R_j = 200\,\mathrm{M\Omega}$) because current was more easily lost into the neuronal network. Adding more layers had very small effects on the responses, so only examination of the raw data could reveal the conditions when stable responses were achieved. The two conditions with $R_j = 4000\,\mathrm{M\Omega}$ showed stable responses at one or more layers. The condition with $R_j = 200$ and $R_n = 15\,\mathrm{M\Omega}$ (R_n is defined as the resistance of a neuron which would correspond to the input resistance when there is no electrical coupling to other cells) showed stable responses at two or more layers. Finally, the condition with $R_j = 200$ and $R_n = 60\,\mathrm{M\Omega}$ showed stable responses at three or more layers. Thus simulations of less than four layers were sufficient to completely reveal the range of voltage responses in coupled cell networks. A total of 1000 networks were simulated with the number of layers uniformly distributed between 1 and 3.

The individual resistances of neurons and gap junctions in these networks were randomized within ranges observed in animal experiments. Published data on nonpyramidal input resistances cannot be used as estimates of neuron resistance because of potential contamination by the effects of junctional coupling between cells which tends to lower input resistance. The input resistances of pyramidal neurons were used as estimates of neuron resistance since these cortical projection neurons do not tend to exhibit coupling to neighboring cells (Deans et al., 2001; Galarreta and Hestrin, 2001; Theis et al., 2003) and therefore the voltage response to current injection reflects the resistance of a single neuron. This is appropriate for the pyramidal neurons and non-pyramidal cells (such as *inhibitory* interneurons) of similar sizes since neuron resistance is inversely proportional to cell size. However, there are some pyramidal neurons which are larger and some nonpyramidal neurons which are smaller (such as *excitatory* granule cells) such that simulating only pyramidal cell data could include lower neuron resistances and potentially exclude some higher neuron resistances but electrical coupling in the cortex appears to be selective for distinct populations of inhibitory interneurons (Alonso, 2002; Miller, 2003). To compensate for the potential exclusion of higher resistances, our simulations included pyramidal cell input resistances during in vitro experiments which express values about twice that observed during in vivo recordings because of reduced synaptic activity. The mean ± SD input

resistances of neocortical pyramidal neurons range from $28.6 \pm 4.2\,M\Omega$ for in vivo recordings during ketamine anesthesia to $37.3 \pm 3.9\,M\Omega$ for in vivo recordings during barbiturate anesthesia and to $66.14 \pm 1.3\,M\Omega$ for in vitro recordings (Pare et al., 1998). By plotting these values, it was observed that the SD values were linearly related to their corresponding mean input resistances, so the following linear regression equation was derived: $SD_{Rn} = 6.7 - 0.08 Mean_{Rn}$, where Rn represents resistance of the neuron. A uniformly distributed random number generator was used to select a mean neuron resistance between 24.5 and 55.5 MΩ and then a normally distributed random number generator (Press et al., 1988) was used to set the resistances for all neurons in the simulation of one network such that the SD of these resistances agreed with the equation for SD_{Rn}. This was repeated 1000 times in order to simulate 1000 networks reflecting a wide range of neuron resistances. Similarly, the mean junctional resistances of these 1000 networks were uniformly distributed between 200 and 4000 MΩ and then the SD of a mean junctional resistance in a single network was set according to $SD_{Rj} = 0.12 Mean_{Rj} + 80.7$ since the reported SD values were found to be linearly related to the mean (Galarreta and Hestrin, 1999; Gibson et al., 1999; Tamas et al., 2000).

The wide range of parameters chosen for the simulated networks would be expected to overlap those of a real network of coupled neurons. The degree of overlap is unknown since accurate data that are not contaminated by the effects of indirect coupling are lacking (i.e. available estimates of both neuron and junctional resistances in networks of coupled cells are contaminated by conductance through neighboring cells). Fortunately, an exact replication is not necessary because the aim is to derive equations that will reveal the junctional and neuron resistances defined in the simulation. Once validated for the simulation data, it should then apply to real intracellular studies of coupled-cells which conform to the architecture of our simulated networks.

3.2. Estimating junctional conductance

The voltage responses to hyperpolarizing stimuli applied successively to either neuron of the pair of recorded neurons embedded within each of the 1000 simulated networks were collected for analyses. The plan was to analyse individual and combined experimental parameters only available from the dual-recorded neurons in order to identify predictors of junctional conductance. Potential combinations of parameters were sought by studying the architecture of networks. It was discovered that a wye–delta circuit conversion (Robbins and Miller, 2000) could be used to simplify the 3D network (Fig. 1) into an equivalent two cell circuit as shown in Fig. 3. This figure shows the simplest network structure (Fig. 3a) which contains all the components of the more complicated 3D network (Fig. 1). This network contains one primary loop (representing a blue cell in Fig. 1) and one secondary loop (representing a transparent cell in Fig. 1) which can be converted using the wye–delta circuit equations (Fig. 3f) into an electrical equivalent pair of coupled cells (Fig. 3e). The resistances of this simplified two cell circuit (Fig. 3e) can be derived from voltage responses to current injection. The derivation is identical whether the two cell circuit represents single cells (i.e. not coupled to surrounding cells) or the summed effects of coupling with neighboring cells. For simplicity, the derivation for single cells will be described (Fig. 4) and then the subscript "p" will be added to the final equations in order to reflect the case where the resistances are the summation of parallel resistances including neighboring cells (Fig. 3e).

A typical experiment involves injecting current into one neuron and recording the voltage changes produced in both neurons (Fig. 4a). A current of I_1 injected into cell 1 will divide to flow along the two existing parallel paths: one through the resistance of cell 1 (R_1) directly to ground and another through the junctional resistance (R_j) and then through the resistance of cell 2 (R_2) to ground (Fig. 4b). The voltage change in cell 1 produced by current injection into this cell (V_{11}) can be derived from Ohm's Law ($V = IR$) with I as the injected current (I_1) and R as the sum of all resistances arranged in series and parallel along the two paths to ground ($1/R_{11} = 1/(R_j + R_2) + 1/R_1$ so $R_{11} = R_1(R_j + R_2)/(R_1 + R_j + R_2)$):

$$V_{11} = I_1 \frac{R_1(R_j + R_2)}{R_1 + R_j + R_2} = I_1 R_{11}. \quad (1)$$

The voltage change in the postsynaptic cell (V_{12}) can also be calculated using Ohm's law with I as the junctional current resulting from current injection into cell 1 and R as the resistance of cell 2 ($V_{12} = I_{1j} R_2$). The value of I_{1j} can be calculated from the division of current I_1 to pass through both the resistance of cell 1 and the resistance through the gap junction and cell 2 ($I_{1j} = I_1(R_1/(R_1 + R_j + R_2))$). Replacing $I_1 j$ in the equation for V_{12} above yields

$$V_{12} = I_1 \frac{R_1 R_2}{R_1 + R_j + R_2} = I_1 R_{12}. \quad (2)$$

The same procedures are used to calculate the voltage responses to current injection into cell 2. This yields the following:

$$V_{22} = I_2 \frac{(R_1 + R_j)R_2}{R_1 + R_j + R_2} = I_2 R_{22}, \quad (3)$$

$$V_{21} = I_2 \frac{R_1 R_2}{R_1 + R_j + R_2} = I_2 R_{21}. \quad (4)$$

The three resistances of the electrotonically coupled cell pair (R_1, R_2 and R_j) are obtained from the simultaneous solution of the three equations derived above (Eqs. (1)–(3)). Eq. (4) can be used instead of Eq. (2) since they are equal during the present conditions. Solving these three simultaneous equations and adding the subscript "p" to indicate that each neuron of the simplified two cell circuit represents the summed contribution of neighboring cells (Fig. 3e)

yields

$$R_{j_p} = \frac{V_{11}V_{22}I_1 - V_{12}^2 I_2}{I_1 I_2 V_{12}}, \quad (5)$$

$$R_{1_p} = \frac{V_{12}^2 I_2 - V_{11}V_{22}I_1}{I_1(I_2 V_{12} - I_1 V_{22})}, \quad (6)$$

$$R_{2_p} = \frac{V_{12}^2 I_2 - V_{11}V_{22}I_1}{I_1 I_2 (V_{12} - V_{11})}. \quad (7)$$

For the sake of completeness, we include the coupling coefficient (K) which is calculated as the postjunctional voltage divided by the prejunctional voltage resulting from prejunctional current injection ($K_{12} = V_{12}/V_{11}$ and $K_{21} = V_{21}/V_{22}$). Unlike the neuron or junctional resistance, this unit-less quantity does not identify a circuit component of coupled cells, so its calculation remains the same whether dual-recorded cells are isolated from other cells or embedded in a network of coupled cells.

To reveal the exact junctional conductance directly linking dual-recorded cells in a network, one would need information from intracellular recordings of surrounding cells. This would be technically challenging. Since electrophysiological studies of coupled cells typically involve dual-cell recordings, our aim was to derive a model using this limited information. To derive a mathematical model of the coupled cell networks simulated with SPICE, we took into consideration the results of previous work (Galarreta and Hestrin, 2001; Rela and Szczupak, 2003) indicating that coupling coefficients between directly coupled pairs are at most 0.2, so indirect coupling would be 0.04 via one intermediate cell and indirect coupling via two intermediate cells would be an insignificant value of 0.008. In order to justify ignoring such higher-order coupling, one needs to show that the drop in coupling is not offset by an increased number of higher-order coupling arranged in parallel. This was shown in Fig. 2 where the voltage responses to current injection were largely due to the addition of the first layer of cells covering the dual-recorded cells. Minimal changes occurred by adding 2 more layers (representing a total of 3 layers formed of 392 neurons and 1603 gap junctions) and undetectable changes occurred with further increases in layers. Therefore, we only considered indirect coupling via single interposed cells (blue cells in Fig. 1a or primary loop in Fig. 3) when modeling the network. The simulations included four of these interposed cells (Fig. 1a) forming four parallel loops that could be summed to produce a single loop as shown in Fig. 3c.

Since we do not have access to electrophysiological parameters from unrecorded neighboring cells during real biological experiments, it was postulated that for equation R_b (Fig. 3f), the junctional resistances could be represented by values $R_x = R_z = R_j/i$ and the membrane resistance

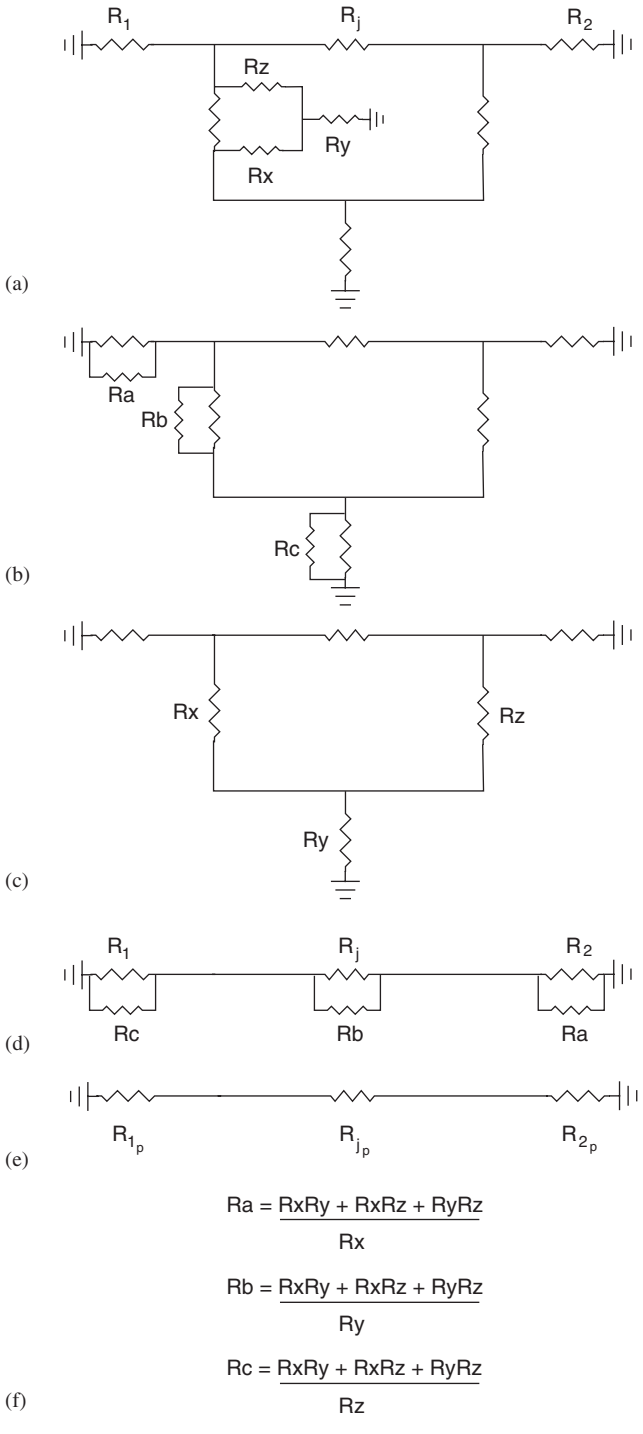

Fig. 3. Method of simplifying a 3D network to an equivalent circuit model of a pair of electrically coupled cells. (a) Sample network configuration based on a subset of the circuit in Fig. 1c containing only one primary and one secondary loop (the secondary loop, identified by R_x, R_y, and R_z, is to be reduced to an equivalent circuit). The dual-recorded neurons are each represented by their individual resistances (R_1 and R_2) and by their junctional resistance (R_j). (b) The result of converting R_x, R_y, and R_z into the parallel resistances R_a, R_b, and R_c using the wye–delta conversion shown in panel (f) below. (c) The summation of parallel resistances in panel (b) to produce the reduced circuit with one primary loop containing new resistances re-labeled R_x, R_y, and R_z. (d) The result of again converting R_x, R_y, and R_z into the new parallel resistances re-labeled R_a, R_b, and R_c. (e) The summation of parallel resistances in panel (d) to produce an equivalent circuit to a pair of coupled cells with resistances R_{1_p}, R_{j_p}, and R_{2_p} where the subscript "p" indicates that the resistances result from the summation of parallel resistances. (f) The wye–delta conversion equations (Robbins and Miller, 2000).

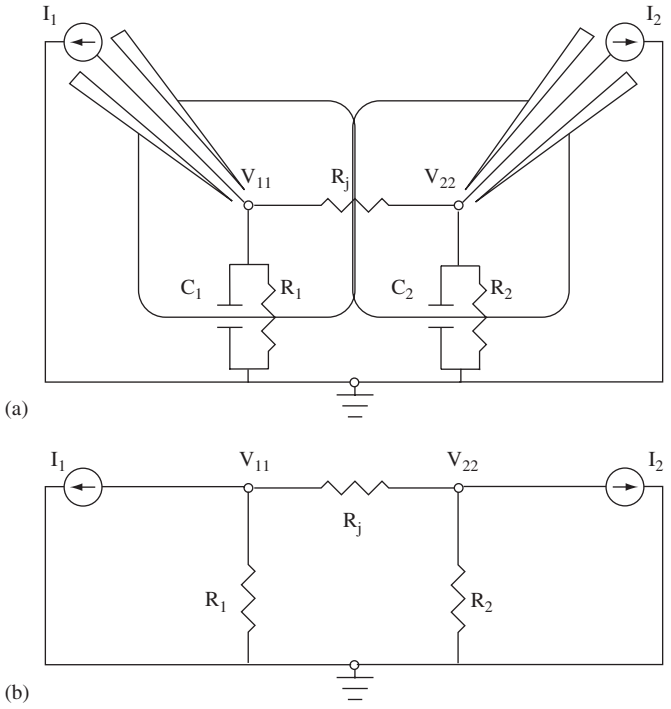

Fig. 4. Basic model of electrotonic coupling via a gap junction linking a pair of recorded cells. (a) Outline of two electrotonically coupled cells each with an intracellular electrode and an overlay of the equivalent circuit model. Note the closed circuit from the electrode tip in the cell to its base representing the ground of the electronic device which is isopotential with the extracellular fluid. (b) Circuit representing coupled-cell model at steady-state which does not require capacitance. This circuit is used for deriving equations. C_1 is the membrane capacitance of cell 1, R_1 is the membrane resistance of cell 1, I_1 is the current injected into cell 1, V_{11} is the voltage in cell 1 in response to current injection into cell 1. These parameters are also defined with respect to cell 2. R_j is the resistance of the gap junction linking the recorded pair of cells.

could be represented by the value $R_y = R_n/i$, where R_j is the junctional resistance directly linking the dual-recorded neurons, R_n is the resistance of a neuron and $i = 4$ interposed neurons forming four parallel primary loops (corresponding to blue cells in Fig. 1a) in the present simulations. Given that the simplification of the 3D network (Fig. 3d,e) produces

$$1/R_{j_p} = 1/R_j + 1/R_b \tag{8}$$

(according to summation of parallel resistances), then expanding R_b in Eq. (8) and solving for R_j yields

$$R_j = 1/2R_{j_p} - R_n + 1/2\sqrt{R_{j_p}^2 + 4R_{j_p}R_n + 4R_n^2 + 4R_{j_p}iR_n}, \tag{9}$$

where the value of R_{j_p} is obtained from Eq. (5) and the value of R_n is estimated from the mean of R_{1_p} and R_{2_p} obtained using Eqs. (6) and (7) (these two parameters are used as estimates of R_n because they most closely reflect properties of recorded cells that are coupled to surrounding cells).

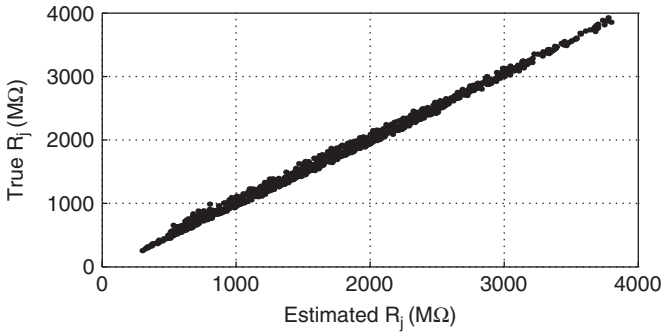

Fig. 5. Estimating junctional resistance between dual-recorded cells embedded in a 3D network of coupled cells. Each dot represents a single data point from the 1000 simulations of networks with randomization of one to three cell layers, neuron resistances from 24.5–55.5 MΩ, and junctional resistances from 200–4000 MΩ. The x-axis contains the estimated junctional resistances using the mathematical model (Eq. (9)). The y-axis contains the true values of the junctional resistances (R_j) defined for the dual-recorded neurons in the simulations.

The accuracy of this mathematical model can be assessed by applying it to recordings from the simulated 3D networks of heterogeneous coupled cells. It can be seen from Fig. 5 that the mathematical model accurately estimated the junctional resistance between dual-recorded cells defined in the 3D networks. Consequently, the mathematical model (Eq. (9)) can be applied to real network dual-cell recordings in order to estimate the junctional resistance or conductance ($1/R_j$) between recorded neurons even though they are embedded in a network of coupled cells. The value of i in Eq. (9) must be determined from anatomical analyses (Bahrey and Moody, 2003; Stewart, 1981) since electrophysiological recordings cannot identify the number of neighboring cells providing parallel primary loops for current flow between the dual-recorded cells (corresponding to $i = 4$ blue cells in Fig. 1a). The error obtained by not accounting for the value of i is shown in Fig. 6 by the exponential decline in R_{j_p} with an increasing number of these parallel primary loops. Remember that the calculations of junctional resistance in previous studies of coupled cell networks, in fact, represent R_{j_p} (Fig. 3) since the calculations are based on the coupling between a pair of cells without taking into account parallel conductances through neighboring cells. Thus previous studies provide accurate values of R_{j_p} but how closely this reflects R_j largely depends on the number of interposed cells (i) forming primary loops.

Once the value of R_j is obtained then the junctional current is simply obtained from the equation $I_j = (V_{post} - V_{pre})/R_j$, where $V_{post} = V_{12}$ and $V_{pre} = V_{11}$ during stimulation of cell 1 and $V_{post} = V_{21}$ and $V_{pre} = V_{22}$ during stimulation of cell 2.

3.3. Estimating membrane conductance

A similar procedure can be used to derive the resistance of a recorded neuron which would equal the input

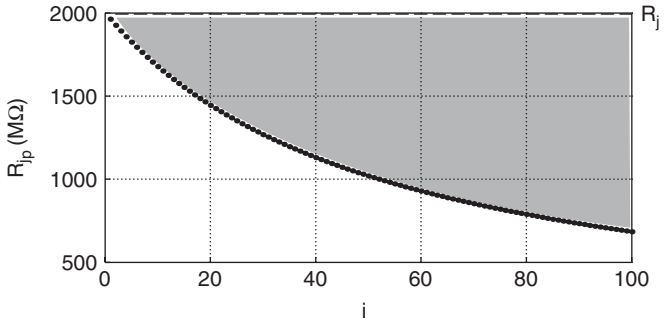

Fig. 6. Effects of increasing the number of primary loops (i) on the combined direct and indirect resistance measured between the dual-recorded cells (R_{j_p}, dotted line) while the direct resistance (R_j, dashed line) remained constant. The shaded area represents the error in calculating junctional resistance when ignoring parallel primary conductance paths through neighboring cells. The relationship between i and R_{j_p} is based on the circuit in Fig. 3c containing one primary loop with resistances R_x, R_y, and R_z. According to the summation of parallel resistances, adding i primary loops is equivalent to a single primary loop with resistances R_x/i, R_y/i, and R_z/i. This primary loop can be simplified such that $1/R_{j_p} = 1/R_j + 1/R_b$ (Fig. 3d,e) where R_b is defined by the wye–delta conversion equation in Fig. 3f. Given all primary loops have values $R_x = R_z = R_j = 2000\,\mathrm{M\Omega}$ and $R_y = 40\,\mathrm{M\Omega}$ then the value of R_{j_p} could be calculated for $i > 0$ (when $i = 0$ then $R_{j_p} = R_j$).

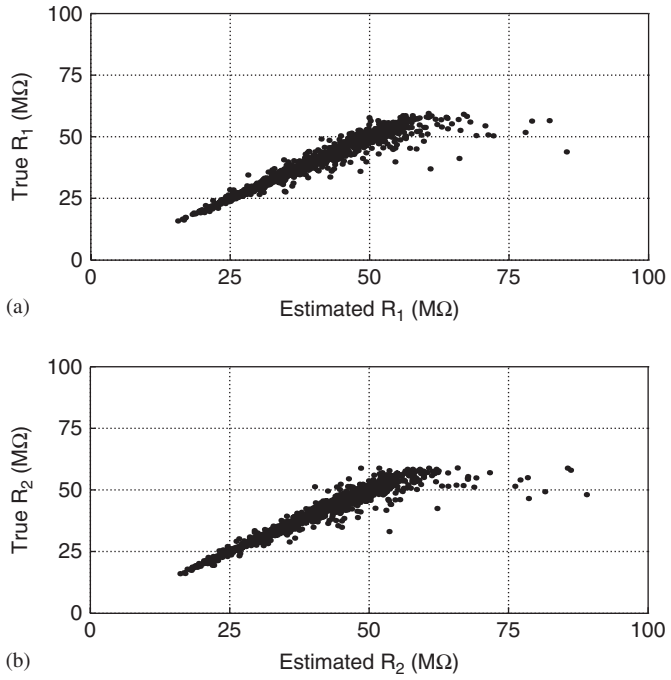

Fig. 7. Estimating resistance of a recorded neuron embedded in a 3D network of coupled cells. (a) Estimation of R_1 using Eq. (10). (b) Estimation of R_2 using Eq. (11). The x-axes contain the estimated neuron resistances and the y-axes contain the true neuron resistances defined for the recorded neurons in the simulations. Each dot represents a single data point from the 1000 simulations of networks with randomization of one to three cell layers, neuron resistances from 24.5–55.5 MΩ, and junctional resistances from 200–4000 MΩ.

resistance in the absence of coupling to neighboring cells. By considering only those neighboring cells directly connected to recorded cell 1 (yellow cell in Fig. 1), current injected into cell 1 would flow to ground directly through the resistance of cell 1 and indirectly through the combined gap junction and neuron resistance of each neighboring cell. Thus the input resistance of the recorded cell would be the sum of the parallel resistances according to the following relation: $1/R_{11} = 1/R_1 + f(1/(R_j + R_n))$, where R_{11} is the input resistance of cell 1 measured as the voltage response divided by the injected current ($V_{11}/I1$), R_1 is the resistance of cell 1 which is sought, f is the number of cells flanking or directly connected to cell 1 (there are 10 such cells for the network in Fig. 1), R_j is the junctional resistance between the recorded cells measured using Eq. (9), and R_n is the resistance of each neighboring cell which is again estimated from the mean of R_{1_p} and R_{2_p} obtained using Eqs. (6) and (7). The value of R_1 can be calculated since all other variables are known. The same procedure would be used to calculate the membrane resistance of cell 2 (R_2), so solving for the membrane resistances of cells 1 and 2 yields

$$R_1 = R_{11}(R_j + R_n)/((R_j + R_n) - fR_{11}), \quad (10)$$

$$R_2 = R_{22}(R_j + R_n)/((R_j + R_n) - fR_{22}). \quad (11)$$

The accuracy of Eqs. (10) and (11) in predicting the true membrane resistances of cells 1 and 2 in each of the 1000 simulated networks is displayed in Fig. 7. The estimates were very accurate except for a few cases of higher neuron resistances. Inspection of the network data revealed that the lower accuracy occurred mostly for networks of one layer of cells and for the combined conditions of high neuron resistances and low gap junction resistances. Such conditions would not be expected to be common in real neural networks of coupled cells.

4. Discussion

This study showed that mathematical modeling could be used to reduce the complexity of a biologically plausible heterogeneous network of coupled neurons to equations that provide relatively accurate estimates of the conductance directly between simultaneously recorded pairs of neurons even though they are embedded in a network of neurons electrotonically coupled by gap junctions. Furthermore, it was possible to extract the resistance provided by an impaled neuron from the input resistance which reflects the sum of parallel resistances through the neuron and neighboring cells. The parameters of these equations only require information available from real dual-intracellular penetrations which allow electrophysiological recordings and intracellular staining. It is expected that more accurate equations could have been derived if one could go beyond the typical limitation of dual-cell recordings and use information from intracellular recordings of neighboring cells with methods derived for inverse problems in electrical networks (Curtis and Morrow, 2000; Strang, 1991).

A critical concept is that input resistance, measured by dividing the voltage response by the injected current,

derives from different components when measured in an isolated neuron as opposed to a coupled neuron. In an isolated neuron, the input resistance is due to the neuron itself whose cell membrane provides resistance to current flow. In a coupled neuron, the input resistance not only reflects the resistance of the impaled neuron but also the sum of the parallel resistances provided by the neighboring cells to which it is electrotonically coupled. Consequently, the steady-state electrical properties during dual-recordings reflect the coupling of either two individual neurons or two populations of neurons. The same equivalent circuit (Fig. 4) and equations (Eqs. (5)–(7)) apply to both situations but the meaning of the results are different. The subscript "p" was added to the equations for representing the coupling of two populations of neurons rather than two individual neurons.

The problem was to reveal the individual neuron properties from dual-recorded neurons embedded in a network of coupled cells which provide indirect conductance via one or more neighboring neurons. A solution to this problem was derived after discovering how the circuitry of the network could be collapsed into an equivalent two cell circuit (Fig. 3). By implementing the reverse process, that is, expanding the two cell circuit (Fig. 3e back to 3d), it was possible to reveal the direct junctional conductance between the dual-recorded neurons and derive its measurement using Eq. (9).

The accuracy of this equation was tested against a simulated 3D network of coupled neurons with heterogeneous electrical properties derived from real neurons. The input resistances of pyramidal cells that were chosen to represent the resistances of neurons do not appear to be contaminated by electrotonic coupling to neighboring cells (Deans et al., 2001; Galarreta and Hestrin, 2001; Theis et al., 2003). However, the gap junction resistances reported and used in the present study (Galarreta and Hestrin, 1999; Gibson et al., 1999; Tamas et al., 2000) represent the variable $1/R_{j_p}$ which is contaminated by indirect conductance through neighboring neurons of the network. The extent of this contamination in the reported gap junction resistances is unknown. Based on Eq. (9) it would largely be dependent on the number of interposed cells (i) forming parallel primary conductance loops (corresponding to blue cells in Fig. 1) between the dual-recorded neurons. This number cannot be revealed from dual-cell recordings and therefore it must be determined from some other means. The most practical method would be to inject intracellular tracers and map its spread through gap junctions into neighboring cells (Bahrey and Moody, 2003; Stewart, 1981) in order to reveal the connectivity of the network and provide an estimate of the number of neurons providing indirect primary conductance paths between the dual-recorded cells. Theoretically, multielectrode recordings could be used to estimate the connectivity of the network but this is either impractical or impossible at the present time. It is for this same reason that the validation of our mathematical models could not be done in live tissue.

Consequently, a simulated 3D network was the best method available to test the accuracy of Eq. (9) in revealing the direct junctional conductance between dual-recorded neurons. As was shown in Fig. 5, this equation provided very accurate estimates. This high level of accuracy was obtained from a simple mathematical model using the voltage responses to current injection in dual-recorded cells and the number of neighboring cells bridging them to form parallel primary conductance loops. Since the voltage responses in neighboring cells are unavailable in dual-cell recordings, the model assumed that the neuron and junctional resistances of the recorded and neighboring cells were a function of the electrical properties of the recorded cells. Despite its conciseness, the model was very accurate in estimating the junctional resistance between recorded cells in networks formed of widely heterogeneous electrical properties. This primarily resulted from the overwhelming contribution of the shortest conductance paths (i.e. parallel primary loops) between the dual-recorded cells. As described in the results, the contribution of indirect conductance paths decreased as the number of constituent cells increased.

A similar modeling approach was used to extract the resistance of the neuron from the input resistance which reflects both the resistance of the neuron and the resistance of the parallel paths through gap junctions leading to neighboring neurons. Here again we used the simplification whereby only the cells directly coupled to a recorded neuron were considered and their resistances were assumed to be a function of the electrical properties of the recorded cells. This led to simple models of the dual-recorded cells (Eqs. (10) and (11)) with a parameter (f) representing the number of flanking neurons (neighboring neurons directly coupled to a recorded neuron) that could be obtained from the same histological analyses mentioned earlier. If gap junction blockers (Jahromi et al., 2002) are very specific and do not affect other channels, then one would expect the input resistances under gap channel block to correspond to the neuron resistances estimated by Eqs. (10) and (11).

The estimated neuron resistances were less accurate at the higher values defined in the networks (Fig. 7). Closer inspection of the networks revealed that the accuracy decreased mostly with one layer of cells and under the combined conditions of high neuron resistances and low gap junction resistances. These combined conditions in the networks likely represent extreme cases rarely observed in real tissue. First, real neurons in a network would most likely be surrounded by more than one layer of cells. Second, the input resistance of neurons tends to decrease as the number of layers increases. Third, the reported values of gap junction resistances, which were used in this study, underestimate the direct junctional resistance between real cells because corrections were not made for the effects of indirect conductance through neighboring cells. Thus the combined conditions of high neuron resistances and low gap junction resistances used in our simulations would not

be expected to be commonly observed in real neural networks.

This mathematical model, which was accurately applied to simulated neurons, should equally apply to real neurons. This is because the steady-state properties of neurons were simulated by their well known electrical equivalents (Bennett, 1966, 1977) using the reliable SPICE software to accurately measure the voltage responses to injected currents. A wide range of biologically relevant parameters were simulated in 1000 neuronal networks with up to three layers of cells surrounding the recorded cell-pair. Such a 3 layered network included 392 cells interconnected by 1603 gap junctions. Therefore the electrical properties of the simulated networks would be expected to overlap the steady-state responses of a real network of coupled cells as long as its features do not fundamentally depart from those in our model. Our model was developed from a 3D mass of coupled cells where dual-recorded cells were found to be largely affected by the single layer of cells surrounding them (Fig. 2) which included the interposed (i) and flanking (f) cells that were used to provide relatively accurate estimates of junctional resistance (R_j) and neuron resistances (R_1 and R_2), respectively. This dominance of the interposed and flanking cells over more distant unrecorded neurons would be due to the exponential drop in current flow through longer cellular paths between the dual-recorded cells because of the high gap junction resistances. These junctional resistances would be expected to be even higher in real neurons than in our simulations which used the published values contaminated by parallel conductances and representing R_{j_p}. Since our model ignored details of the connectivity of other unrecorded cells in a simulated network, the fundamental features to identify in real networks would be the interposed and flanking neurons. Assuming the numbers of interposed (i) and flanking (f) cells do not vary significantly within the same tissue, these values could be obtained in separate experiments to the ones providing the electrophysiological data. Otherwise, tracer injections could be made directly into the recorded neurons. An important assumption of our model was that all cells of a coupled network were isopotential at rest. This is reasonable under conditions where there are no membrane potential changes from pacemaker or synaptic conductances. Otherwise, the effects of differences in resting potential are especially important at high gap junction resistances in isolated pairs of coupled cells (Veenstra, 2001) and possibly also in coupled cell networks. Similarly, our model assumed that the hyperpolarizing stimulus did not trigger voltage-dependent conductances since these would confound the resistance estimates. Furthermore, our model assumed that gap junctions were at their typical location in cell bodies of dual-recorded cells. The effects of gap junctions in neuron branches on estimates of junctional resistance has not yet been examined for dual-recorded cells alone, as defined previously (Bennett, 1966, 1977), or for cells embedded in a network of coupled cells. The effects of such fundamental departures from our model on estimates of the electrical properties of coupled cell networks are open to future work.

One interesting future prospect for revealing properties of coupled cell networks is the evolving technology of optical mapping of electrical activity in brain slice preparations (Grinvald and Hildesheim, 2004; Mochida et al., 2001; Schemann et al., 2002). This imaging is based on voltage-sensitive dyes which bind to the external surface of cell membranes and transform changes in membrane potential into optical signals that provide high spatial and temporal resolution of electrical activity (Grinvald and Hildesheim, 2004). From Figs. 1 and 3, it can be seen that derivation of R_1, R_2 and R_j required a description of the resistances in the network. Optical signals provide an indirect measurement of intracellular voltage but this can only be converted into resistance if some measurements or assumptions on current flow are made. Nevertheless, optical mapping could at least provide some qualitative measure of the relative accuracy with which our model could estimate electrical properties of coupled cell networks. The range of estimated values for any single true value in Figs. 5 and 7 is due to the heterogeneous properties of a simulated network being estimated by a model which assumes homogeneous properties. If unrecorded neurons in the simulations were truly homogeneous then there would have been a tight match between true and estimated values. Homogeneity of electrical properties would be expected to yield optical responses that exhibit an even drop in amplitude with distance from a stimulated cell. Whether the distribution of optical responses could provide a qualitative measure of the relative accuracy of estimated resistances would depend on the ability of the optical technology to accurately resolve the intracellular activity of individual cells in the network. It could be difficult for a 2-D optical sensor to resolve activity from a 3-D network of cells since there is the theoretical possibility that the signal derives from the sum of several underlying cells. Further studies would be required to clarify many of these uncertainties.

In conclusion, biologically realistic networks were simulated and used to derive mathematical models that provided relatively accurate estimates of the resistances of dual-recorded neurons and of the junctional resistance directly linking them. The procedure essentially involved applying Eqs. (5)–(7) and then incorporating the results into Eqs. (9)–(11). An accompanying browser-based program (`http://slice.med.uottawa.ca/public/GapA1Pgm`) is provided to simplify use of these equations in estimating neuron and junctional resistances from dual-cell recording data.

Acknowledgements

This work was made possible from support by the University of Ottawa and the Canadian Institutes of Health Research as well as from discussions with Drs.

Andre Dabrowski and Michel Désilets of the University of Ottawa.

References

Alonso, J.M., 2002. Neural connections and receptive field properties in the primary visual cortex. Neuroscientist 8, 443–456.

Amitai, Y., Gibson, J.R., Beierlein, M., Patrick, S.L., Ho, A.M., Connors, B.W., Golomb, D., 2002. The spatial dimensions of electrically coupled networks of interneurons in the neocortex. J. Neurosci. 22, 4142–4152.

Bahrey, H.L., Moody, W.J., 2003. Voltage-gated currents, dye and electrical coupling in the embryonic mouse neocortex. Cereb. Cortex 13, 239–251.

Bennett, M.V., 1966. Physiology of electrotonic junctions. Ann. N.Y. Acad. Sci. 137, 509–539.

Bennett, M.V., 1977. Electrical transmission: a functional analysis and comparison to chemical transmission. In: Brookhart, J.M., Mountcastle, V.B. (Eds.), Handbook of Physiology, Section 1. The Nervous System, Part I. American Physiological Society, Bethesda, Maryland, pp. 357–416.

Bennett, M.V., 1997. Gap junctions as electrical synapses. J. Neurocytol. 26, 349–366.

Clapham, D.E., Shrier, A., DeHaan, R.L., 1980. Junctional resistance and action potential delay between embryonic heart cell aggregates. J. Gen. Physiol. 75, 633–654.

Curtis, E.B., Morrow, J.A., 2000. Inverse Problems for Electrical Networks. Applied Mathematics. World Scientific, London, vol. 13, pp. 1–180.

Deans, M.R., Gibson, J.R., Sellitto, C., Connors, B.W., Paul, D.L., 2001. Synchronous activity of inhibitory networks in neocortex requires electrical synapses containing connexin36. Neuron 31, 477–485.

Elenes, S., Martinez, A.D., Delmar, M., Beyer, E.C., Moreno, A.P., 2001. Heterotypic docking of Cx43 and Cx45 connexons blocks fast voltage gating of Cx43. Biophys. J. 81, 1406–1418.

Galarreta, M., Hestrin, S., 1999. A network of fast-spiking cells in the neocortex connected by electrical synapses. Nature 402, 72–75.

Galarreta, M., Hestrin, S., 2001. Electrical synapses between GABA-releasing interneurons. Nat. Rev. Neurosci. 2, 425–433.

Galarreta, M., Hestrin, S., 2002. Electrical and chemical synapses among parvalbumin fast-spiking GABAergic interneurons in adult mouse neocortex. Proc. Natl Acad. Sci. 99, 12438–12443.

Gibson, J.R., Beierlein, M., Connors, B.W., 1999. Two networks of electrically coupled inhibitory neurons in neocortex. Nature 402, 75–79.

Grinvald, A., Hildesheim, R., 2004. VSDI: a new era in functional imaging of cortical dynamics. Nat. Rev. Neurosci. 5, 874–885.

Jahromi, S.S., Wentlandt, K., Piran, S., Carlen, P.L., 2002. Anticonvulsant actions of gap junctional blockers in an in vitro seizure model. J. Neurophysiol. 88, 1893–1902.

Marder, E., 1998. Electrical synapses: beyond speed and synchrony to computation. Curr. Biol. 8, R795–R797.

Miller, K.D., 2003. Understanding layer 4 of the cortical circuit: a model based on cat V1. Cereb. Cortex 13, 73–82.

Mochida, H., Sato, K., Sasaki, S., Yazawa, I., Kamino, K., Momose-Sato, Y., 2001. Effects of anisomycin on LTP in the hippocampal CA1: long-term analysis using optical recording. Neuroreport 12, 987–991.

Neyton, J., Trautmann, A., 1985. Single-channel currents of an intercellular junction. Nature 317, 331–335.

Pare, D., Shink, E., Gaudreau, H., Destexhe, A., Lang, E.J., 1998. Impact of spontaneous synaptic activity on the resting properties of cat neocortical pyramidal neurons in vivo. J. Neurophysiol. 79, 1450–1460.

Press, W.H., Flannery, B.P., Teukolsky S.A., Vetterling W.T., 1988. Numerical Recipes in C. Cambridge University Press, New York, pp. 204–241.

Rela, L., Szczupak, L., 2003. Coactivation of motoneurons regulated by a network combining electrical and chemical synapses. J. Neurosci. 23, 682–692.

Robbins, A.H., Miller, W., 2000. Circuit Analysis: Theory and Practice, second ed., Thomson Learning, Florence, Kentucky, pp. 296–299.

Rouach, N., Avignone, E., Meme, W., Koulakoff, A., Venance, L., Blomstrand, F., Giaume, C., 2002. Gap junctions and connexin expression in the normal and pathological central nervous system. Biol. Cell. 94, 457–475.

Rozental, R., Giaume, C., Spray, D.C., 2000. Gap junctions in the nervous system. Brain. Res. Brain. Res. Rev. 32, 11–15.

Schemann, M., Michel, K., Peters, S., Bischoff, S.C., Neunlist, M., 2002. Cutting-edge technology. III. Imaging and the gastrointestinal tract: mapping the human enteric nervous system. Am. J. Physiol. Gastrointest. Liver. Physiol. 282, G919–G925.

Simon, A.M., Goodenough, D.A., 1998. Diverse functions of vertebrate gap junctions. Trends. Cell. Biol. 8, 477–483.

Spray, D.C., Harris, A.L., Bennett, M.V., 1981. Equilibrium properties of a voltage-dependent junctional conductance. J. Gen. Physiol. 77, 77–93.

Stewart, W.W., 1981. Lucifer dyes—highly fluorescent dyes for biological tracing. Nature 292, 17–21.

Strang, G., 1991. Inverse problems and derivatives of determinants. Arch. Rational Mech. Anal. 114, 255–265.

Tamas, G., Buhl, E.H., Lorincz, A., Somogyi, P., 2000. Proximally targeted GABAergic synapses and gap junctions synchronize cortical interneurons. Nat. Neurosci. 3, 366–371.

Theis, M., Sohl, G., Speidel, D., Kuhn, R., Willecke, K., 2003. Connexin43 is not expressed in principal cells of mouse cortex and hippocampus. Eur. J. Neurosci. 18, 267–274.

Veenstra, R.D., 2001. Voltage clamp limitations of dual whole-cell gap junction current and voltage recordings. I. Conductance measurements. Biophys. J. 80, 2231–2247.